

SUPPORTING INFORMATION

Luminescent Cu₄I₄-cubane clusters based on *N*-methyl-5,10-dihydrophenarsazines

Milyausha F. Galimova,^[a] Ekaterina M. Zueva,^[b] Alexey B. Dobrynin,^[a] Ilya E. Kolesnikov,^[c]
Rustem R. Musin,^[b] Elvira I. Musina,^[a] Andrey A. Karasik^[a]

^a Arbuzov Institute of Organic and Physical Chemistry, FRC Kazan Scientific Center, Russian Academy of Sciences, 8 Arbuzov Street, Kazan 420088, Russian Federation

^b Kazan National Research Technological University, 68 Karl Marx Street, Kazan 420015, Russian Federation

^c Center for Optical and Laser Materials Research, Saint Petersburg State University, 5 Ulianovskaya Street, Saint Petersburg 198504, Russian Federation

Table of contents

I. ¹ H NMR spectra of ligands and complexes (Figures S1, S2).....	S2
II. Single-crystal and powder X-ray diffraction data (Tables S1, S2 and Figures S3–S6).....	S3
III. Photophysical properties (Figures S7–S14, Table S3).....	S7

I. ^1H NMR spectra of ligands and complexes

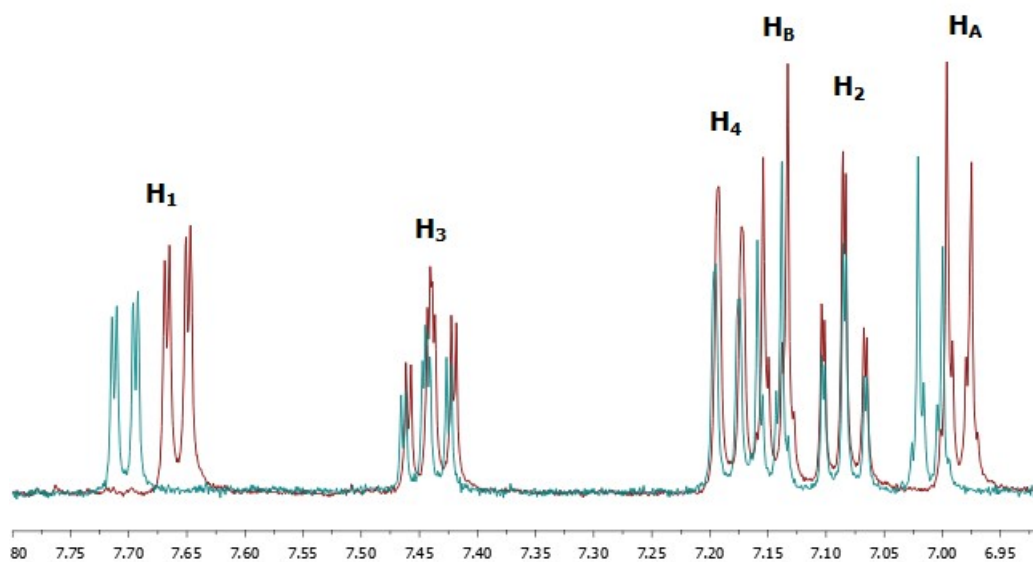


Figure S1. Comparison of ^1H NMR spectra for ligand **1** (red line) and complex **3** (green line), measured in CD_3CN (the range from 6.90 to 7.80 ppm is shown).

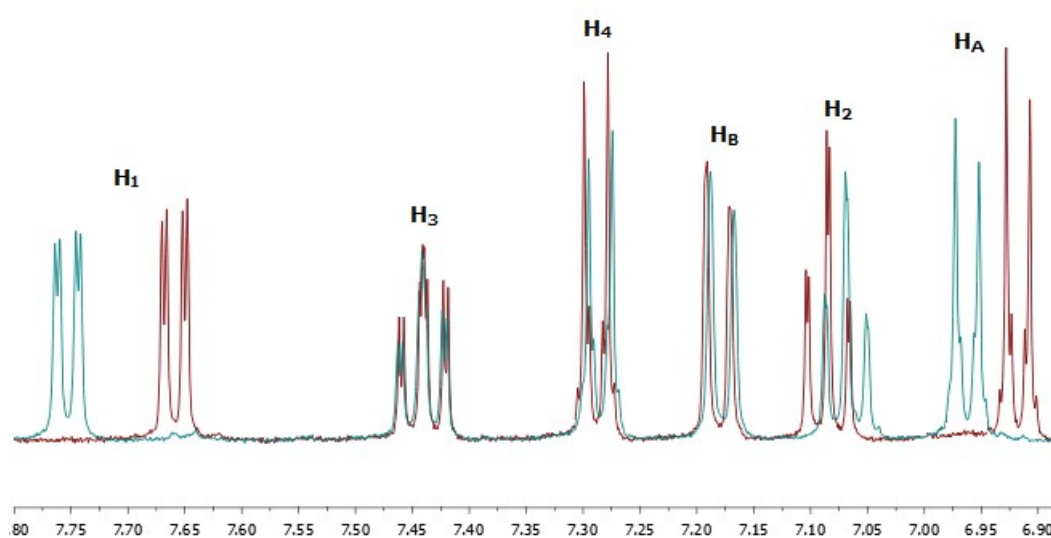


Figure S2. Comparison of ^1H NMR spectra for ligand **2** (red line) and complex **4** (green line), measured in CD_3CN (the range from 6.90 to 7.80 ppm is shown).

II. Single crystal and powder X-ray diffraction data

Table S1. Selected interatomic distances (in Å) in **3** and **4**.

	Complexes	
	3	4
Cu-Cu	Cu1-Cu1 2.678(1)	Cu1-Cu1 2.629(1)
	Cu1-Cu1 2.806(2)	Cu1-Cu1 2.743(2)
	Cu1-Cu1 2.806(2)	Cu1-Cu1 2.743(2)
	Cu1-Cu1 2.806(2)	Cu1-Cu1 2.743(2)
	Cu1-Cu1 2.806(2)	Cu1-Cu1 2.743(2)
Cu-I	Cu1-Cu1 2.687(1)	Cu1-Cu1 2.629(1)
	Cu1-I1 2.652(1)	Cu1-I1 2.652(1)
	Cu1-I1 2.688(1)	Cu1-I1 2.680(1)
	Cu1-I1 2.716(1)	Cu1-I1 2.705(1)
	Cu1-I1 2.652(1)	Cu1-I1 2.652(1)
	Cu1-I1 2.688(1)	Cu1-I1 2.680(1)
	Cu1-I1 2.716(1)	Cu1-I1 2.705(1)
	Cu1-I1 2.652(1)	Cu1-I1 2.652(1)
	Cu1-I1 2.688(1)	Cu1-I1 2.680(1)
	Cu1-I1 2.716(1)	Cu1-I1 2.705(1)
	Cu1-I1 2.652(1)	Cu1-I1 2.652(1)
Cu-As	Cu1-As1 2.362(1)	Cu1-As1 2.353(1)
	Cu1-As1 2.362(1)	Cu1-As1 2.353(1)
	Cu1-As1 2.362(1)	Cu1-As1 2.353(1)
	Cu1-As1 2.362(1)	Cu1-As1 2.353(1)
	Cu1-As1 2.362(1)	Cu1-As1 2.353(1)

Table S2. Selected structural parameters (distances in Å, angles in °) for **3** and **4**.

	Complexes	
	3	4
As1... <i>P</i> (C1C6C7C12)	0.636	0.629
N1... <i>P</i> (C1C6C7C12)	0.388	0.378
As1...C13	1.959	1.946
∠C13-As1-C1	97.74	97.39
∠C13-As1-C12	100.64	100.40
∠C1-As1-C12	94.88	95.74
∠C6-N1-C7	121.12	122.21
∠ <i>P</i> (C1-C6)- <i>P</i> (C7-C12)	37.75	35.24
∠ <i>P</i> (C1C6C7C12)- <i>P</i> (C13-C18)	76.79	76.93
∠N1-As1-C13-C14(C18)	72.79	71.97

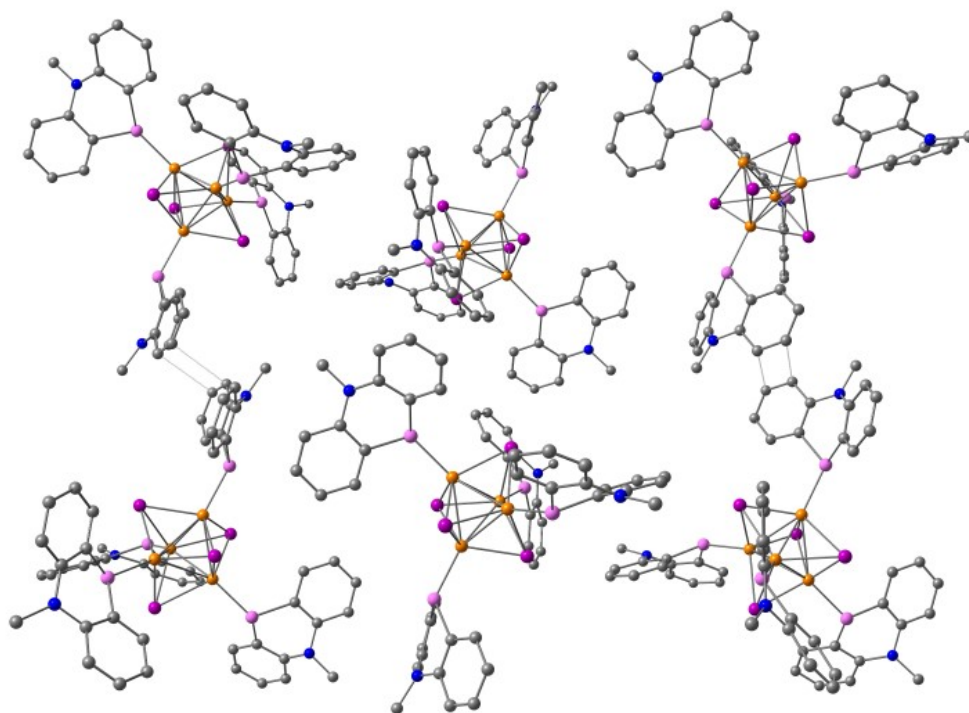


Figure S3. Fragment of packing of **3** in the crystal. The aryl substituent at the arsenic atom is not shown for clarity. Similar packing is observed for **4**.

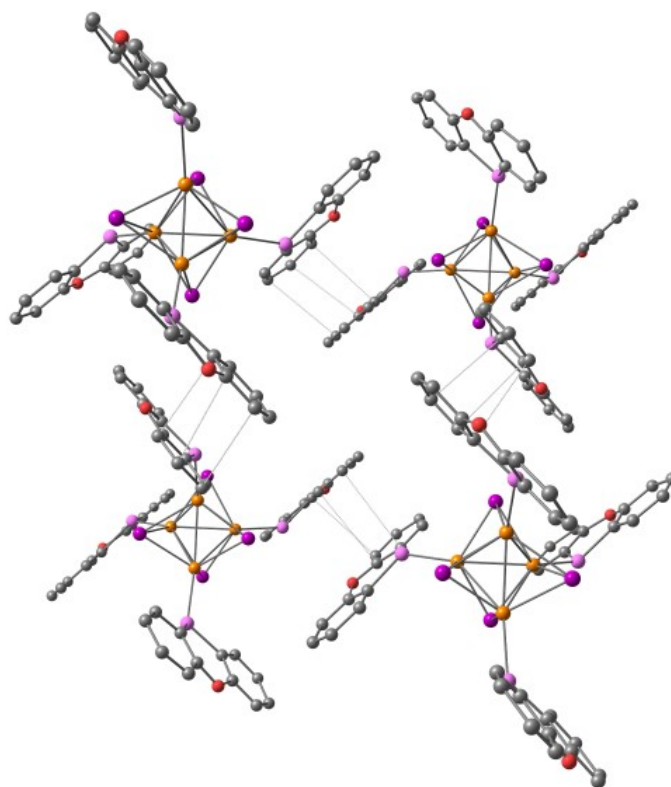


Figure S4. Fragment of packing of compound $[\text{Cu}_4\text{I}_4(10\text{-}p\text{-fluorophenyl)phenoxarsine}]_4$ in the crystal. The aryl substituent at the arsenic atom is not shown for clarity.

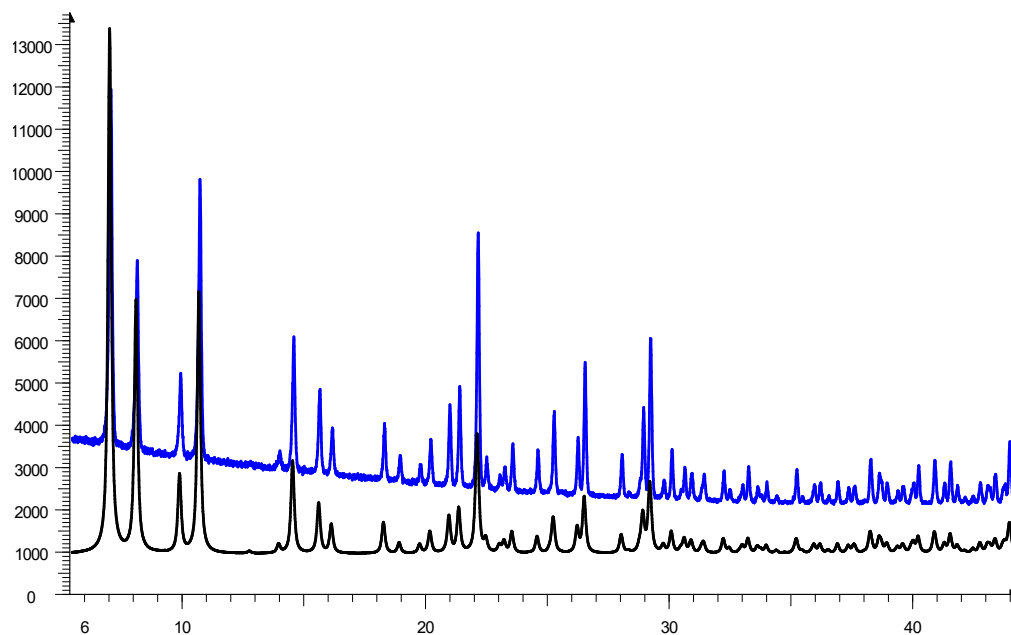


Figure S5. Theoretical powder diffractogram (black line) calculated from the single-crystal X-ray data for **3** and experimental powder diffractogram (blue line) of the dried polycrystalline powder sample.

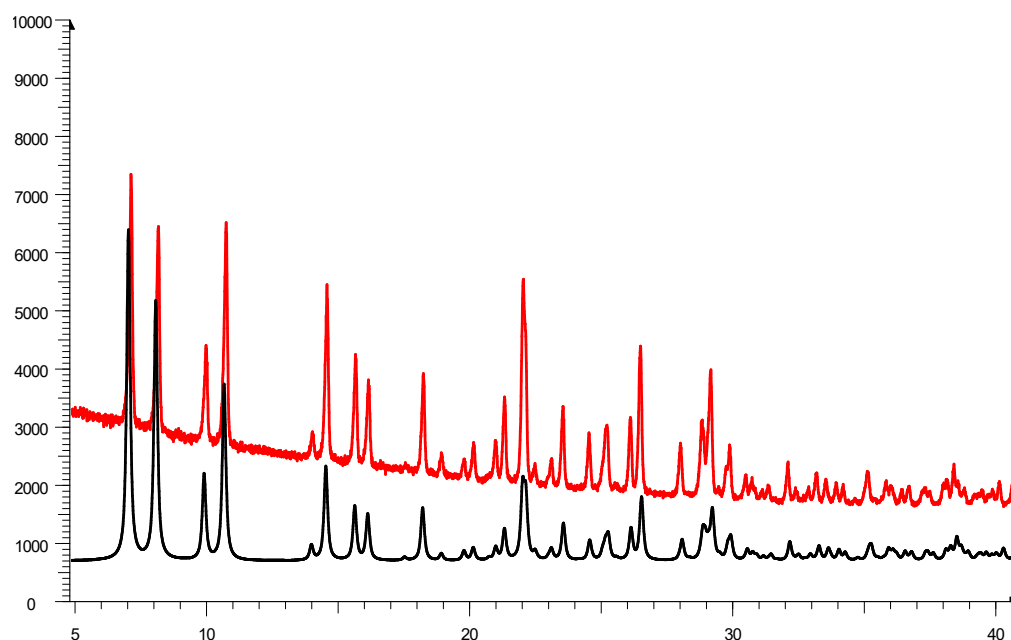


Figure S6. Theoretical powder diffractogram (black line) calculated from the single-crystal X-ray data for **4** and experimental powder diffractogram (red line) of the dried polycrystalline powder sample.

III. Photophysical properties

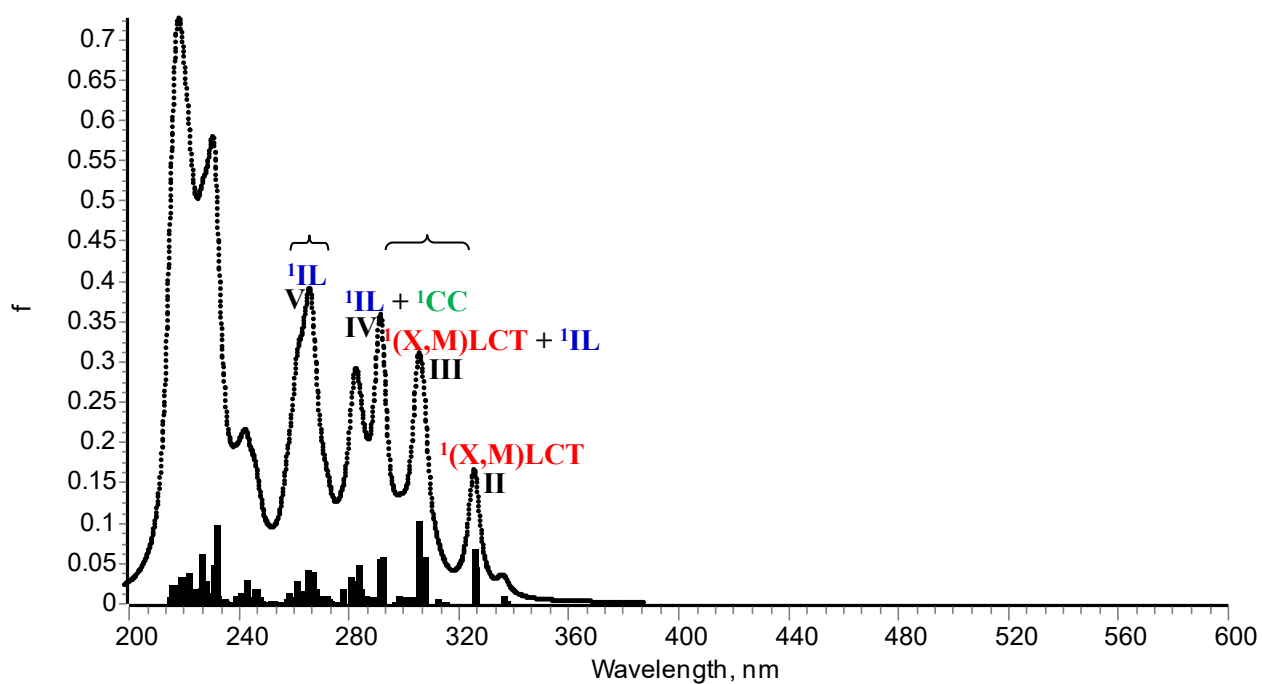
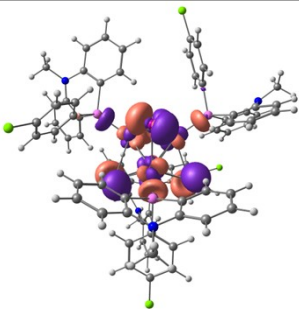
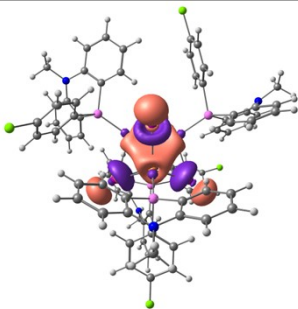
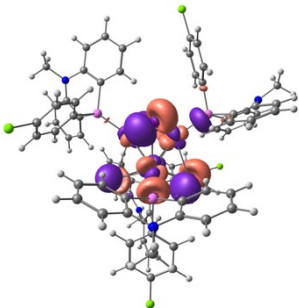
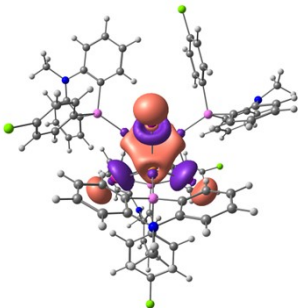
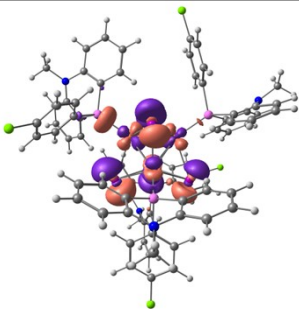
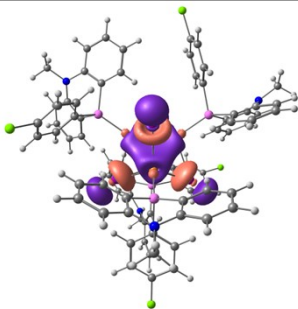
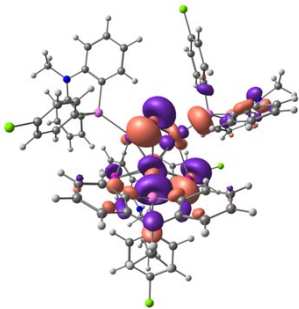
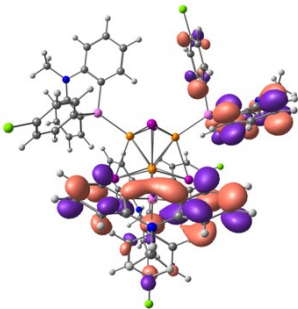
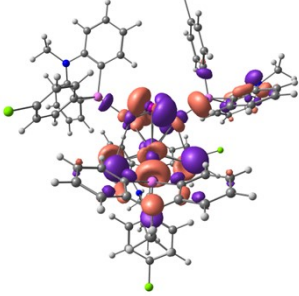
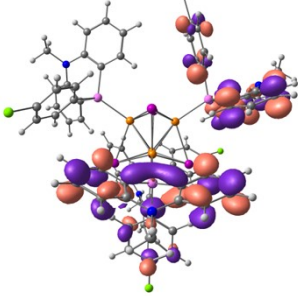
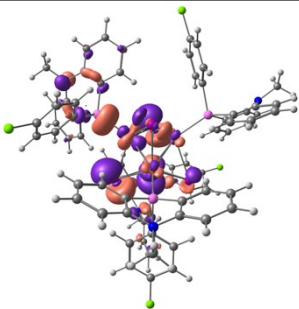
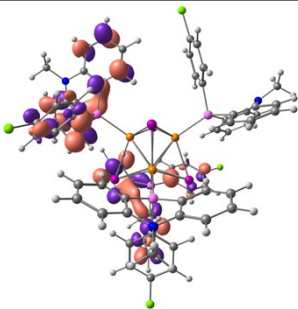
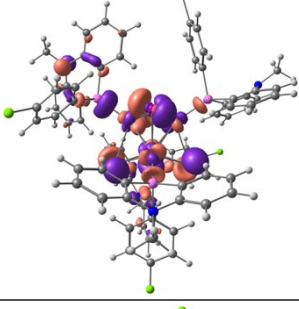
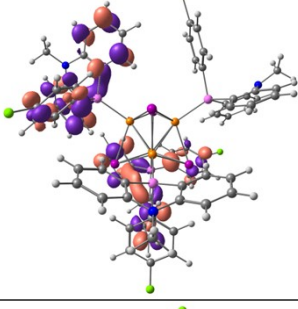
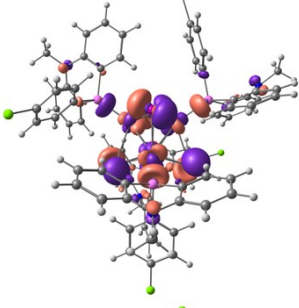
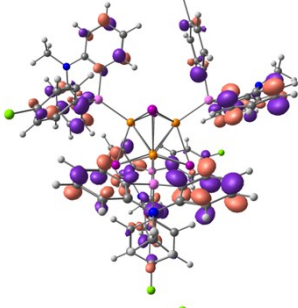
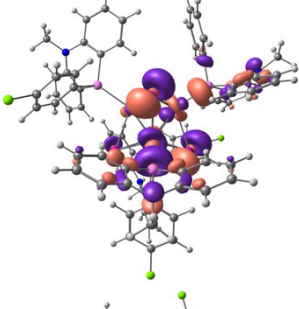
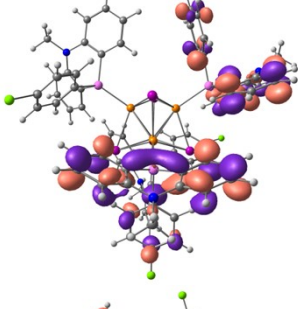
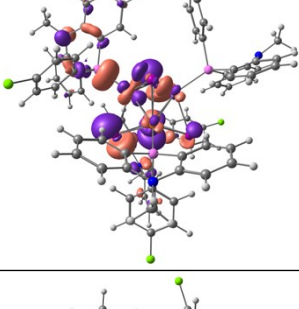
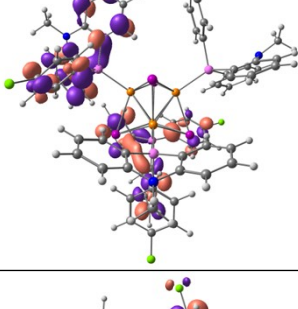
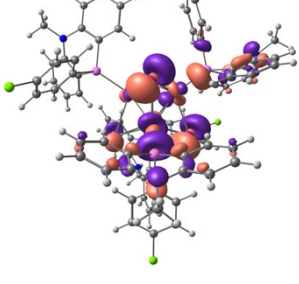
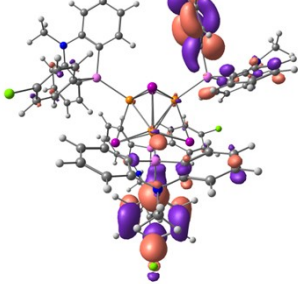
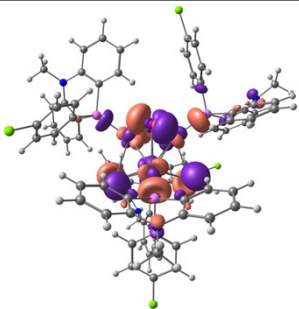
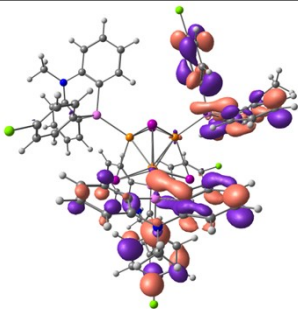
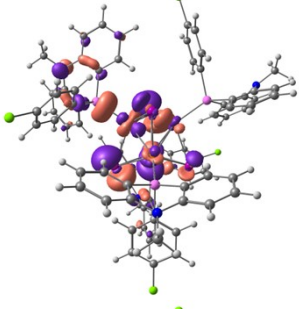
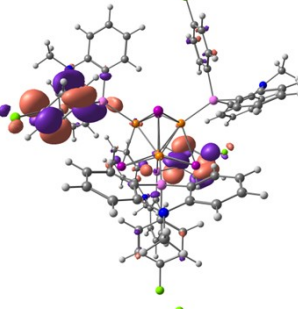
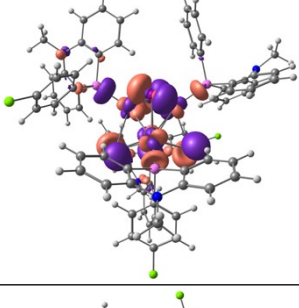
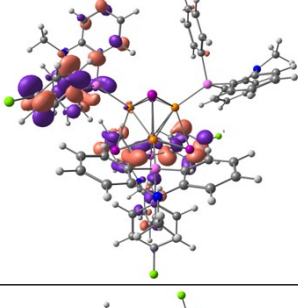
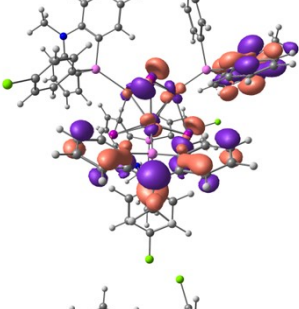
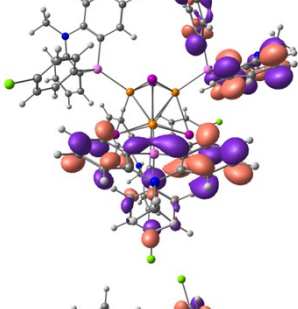
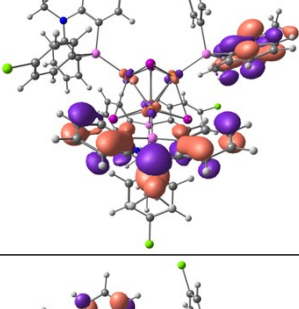
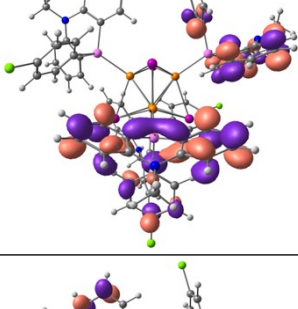
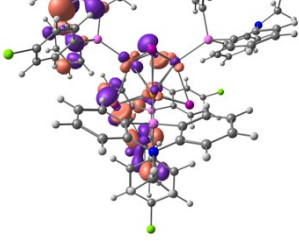
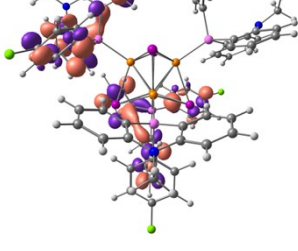


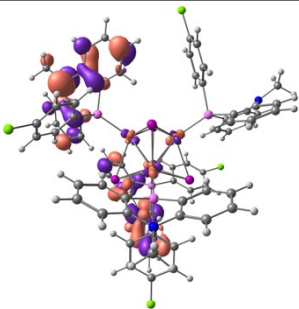
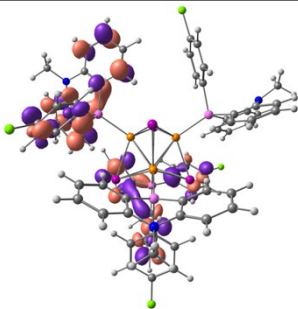
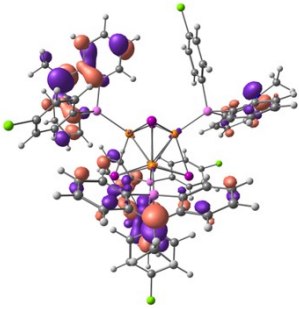
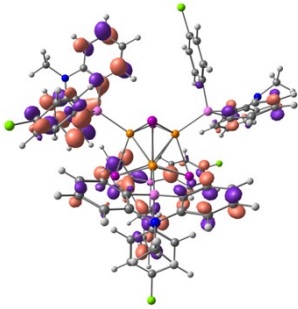
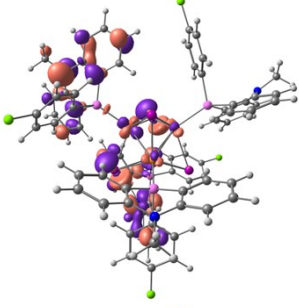
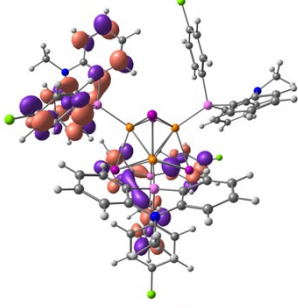
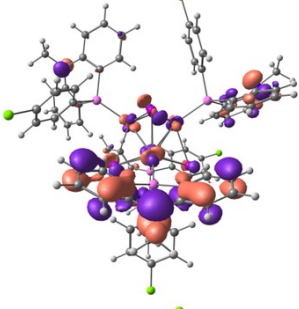
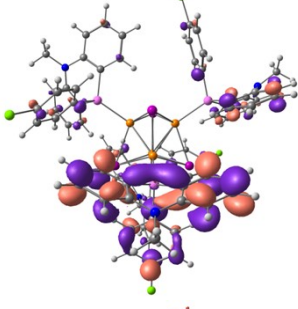
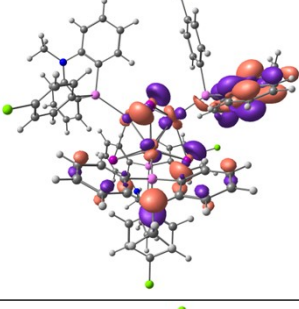
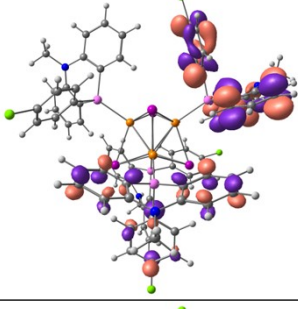
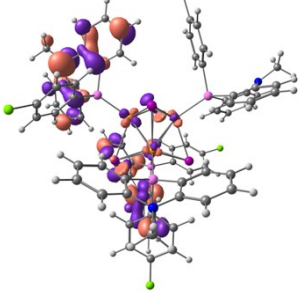
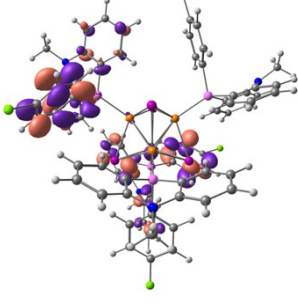
Figure S7. The calculated absorption spectrum for **3**. The vertical lines showing the position of singlet-singlet electronic transitions and their intensity (f – oscillator strength) were broadened by the Lorentz function (f.w.h.m. = 0.25 eV).

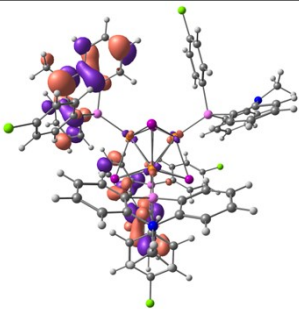
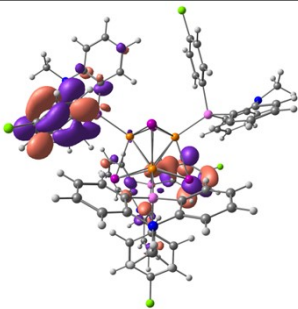
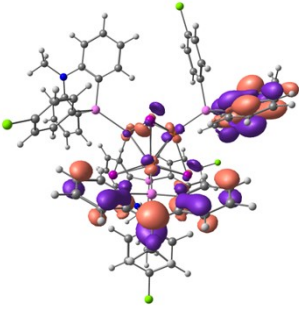
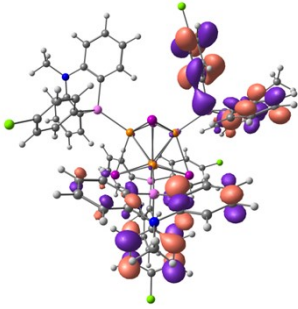
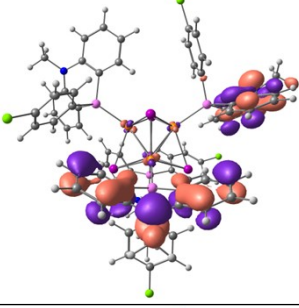
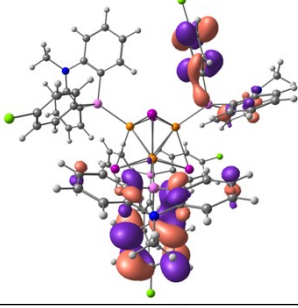
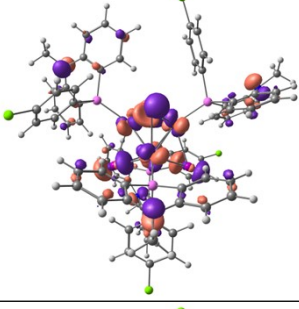
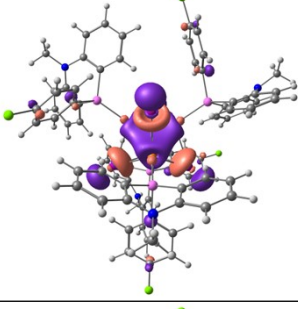
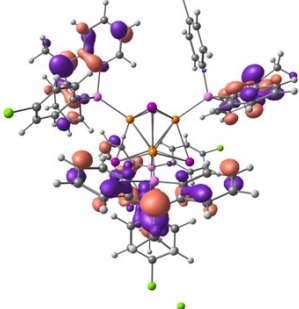
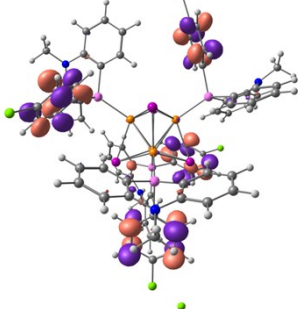
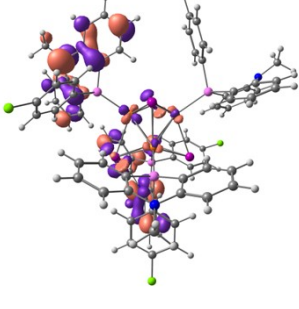
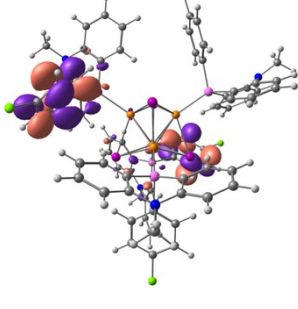
Table S3. The calculated excitation energies (absorption wavelengths), oscillator strengths, natural transition orbital (NTO) pairs and their eigenvalues (occupations) for selected excited states of **3**.

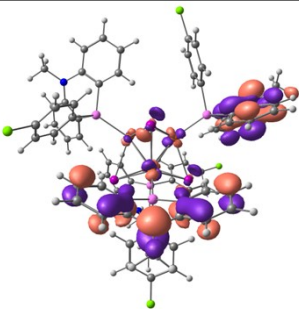
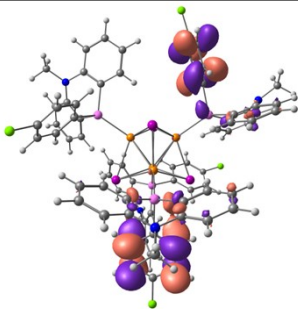
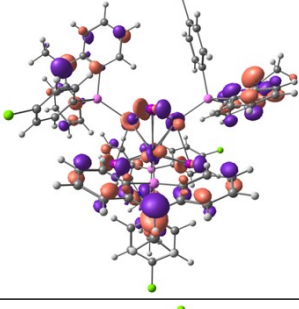
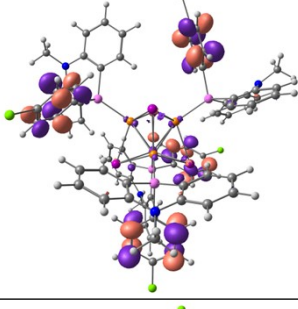
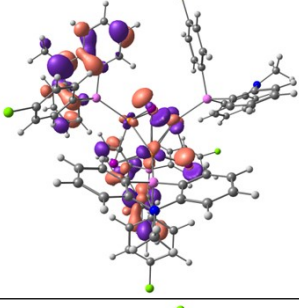
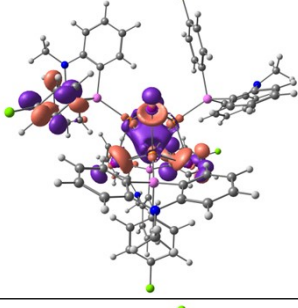
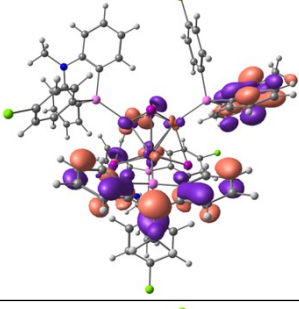
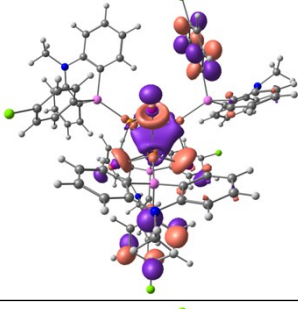
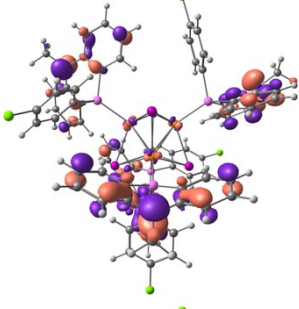
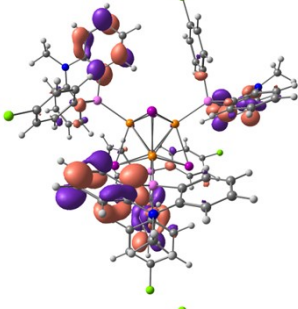
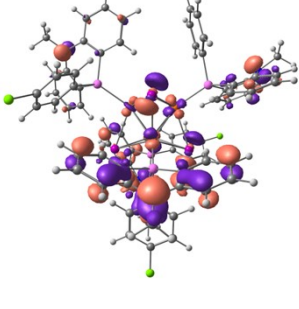
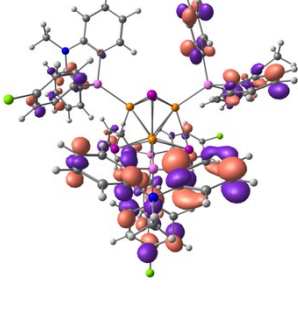
subset: type	λ	f	N_e	occ.	NTO pair	
I: ^1CC	337	0.00	1	0.98		
					HOMO	LUMO+4
	336	0.01	2	0.98		
					HOMO-1	LUMO+4
	336	0.01	3	0.98		
					HOMO-2	LUMO+4
II: $^1(\text{X},\text{M})\text{LCT}$	326	0.05	4	0.70		
						
				0.29		

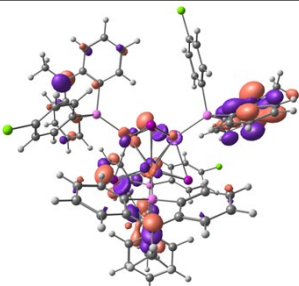
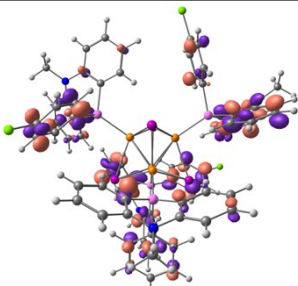
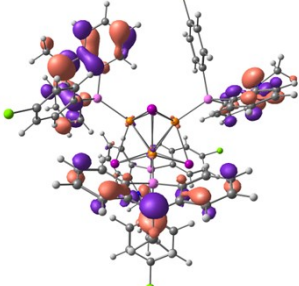
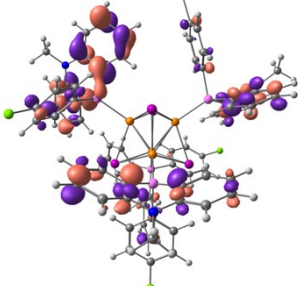
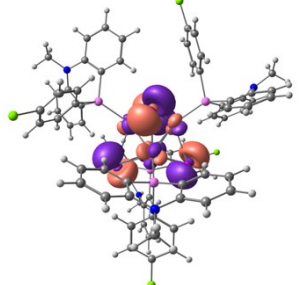
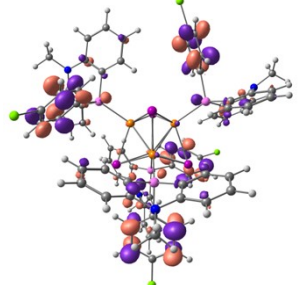
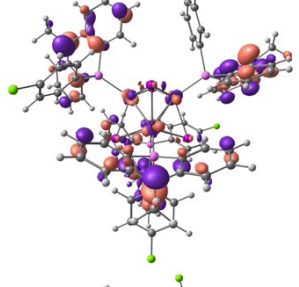
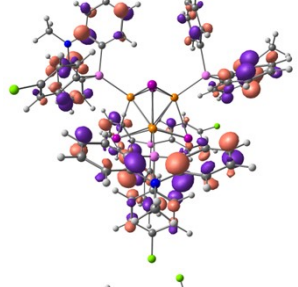
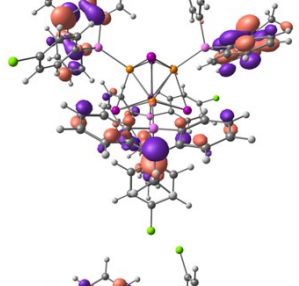
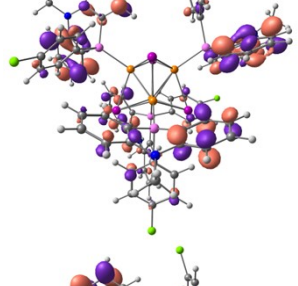
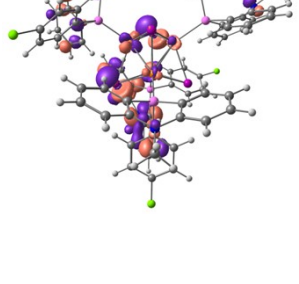
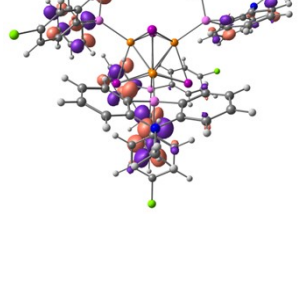
	326	0.05	5	0.70		
				0.29		
	325	0.07	6	0.43		
				0.27		
				0.26		
III: ${}^1(X,M)LCT$ + 1IL	307	0.06	21	0.44		

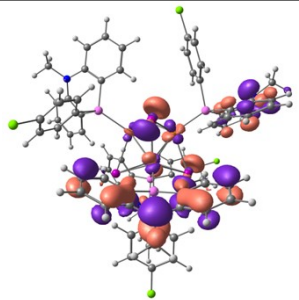
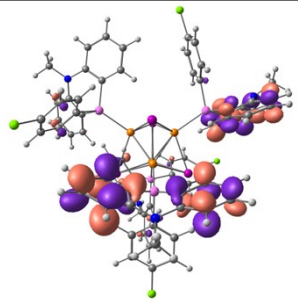
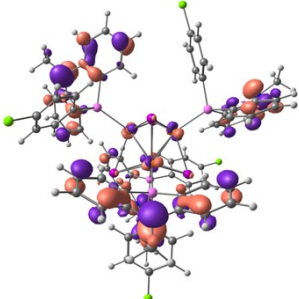
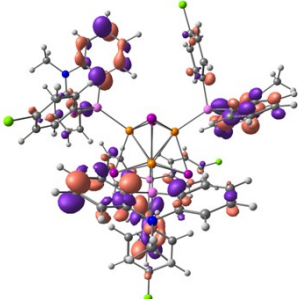
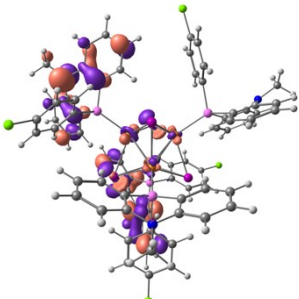
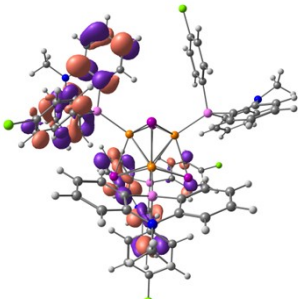
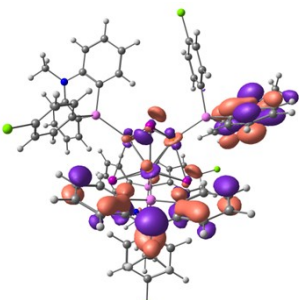
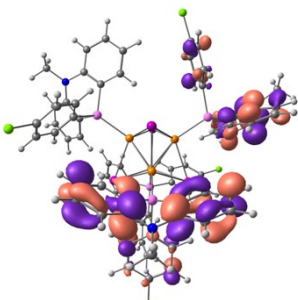
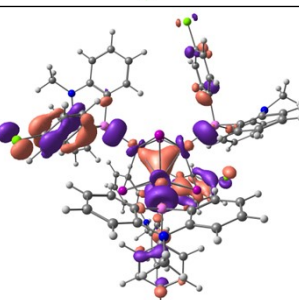
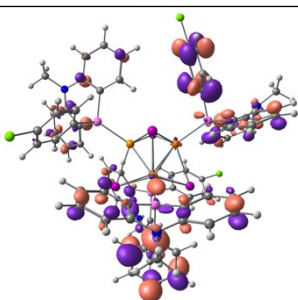
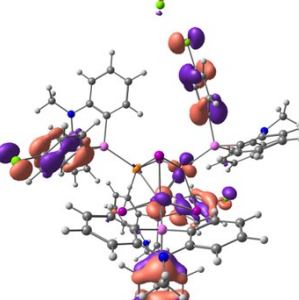
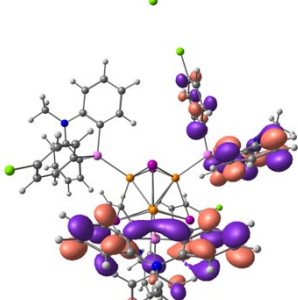
			0.37		
307	0.06	22	0.44		
			0.37		
305	0.05	24	0.45		
			0.30		
305	0.05	25	0.45		

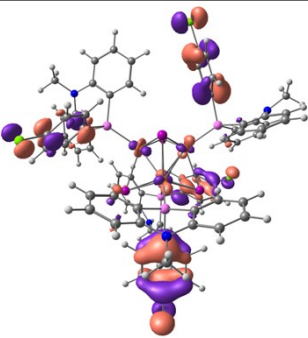
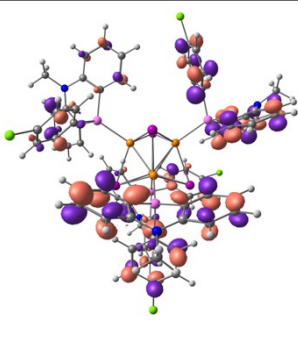
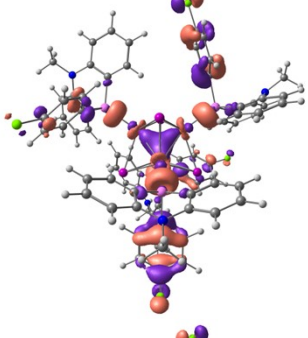
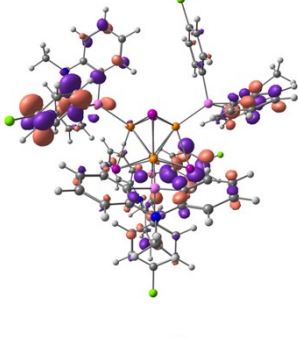
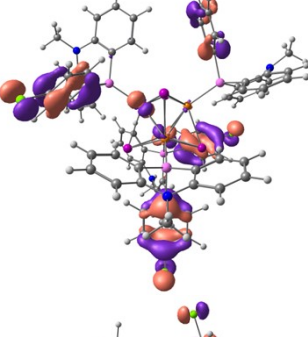
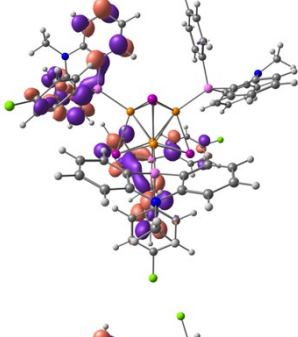
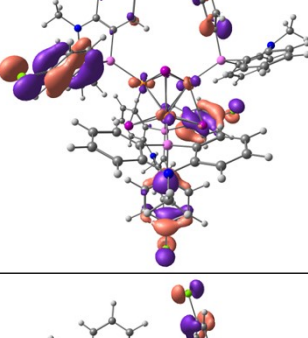
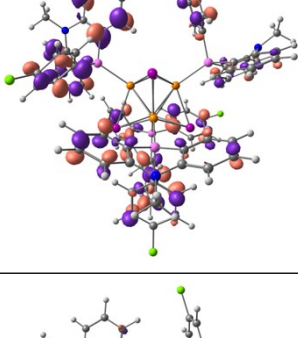
				0.30		
	305	0.10	27	0.24		
				0.21		
				0.20		
				0.20		
IV: ¹ IL + ¹ CC	292	0.06	51	0.55		

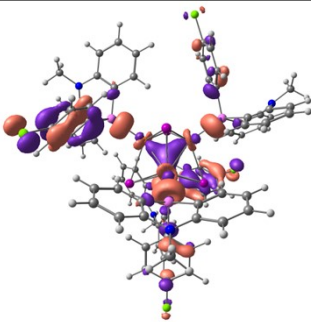
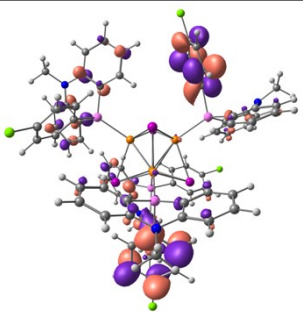
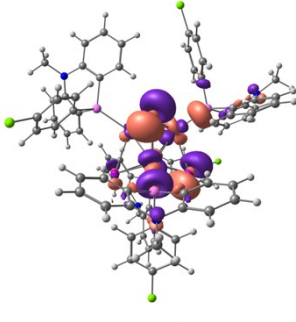
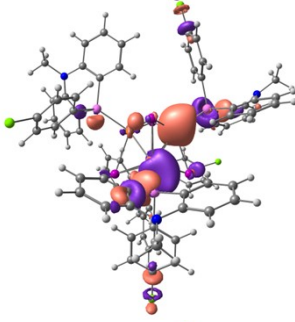
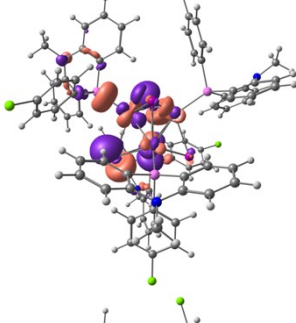
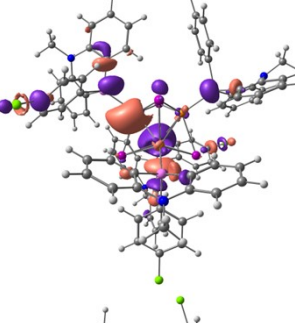
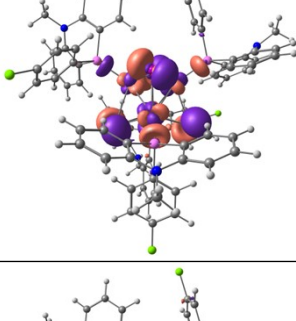
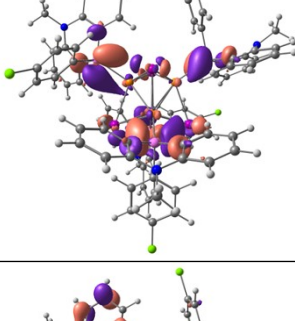
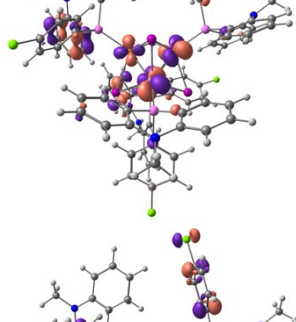
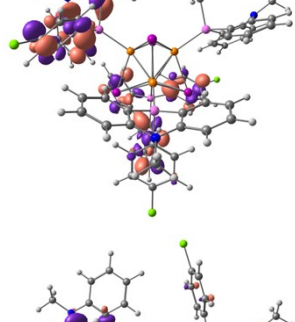
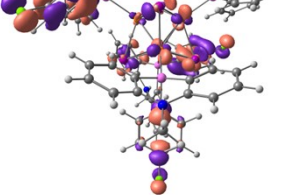
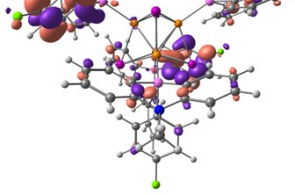
			0.38		
292	0.06	52	0.55		
			0.38		
292	0.04	53	0.63		
291	0.04	54	0.37		
			0.22		

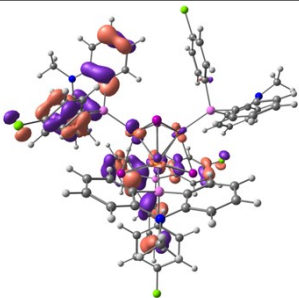
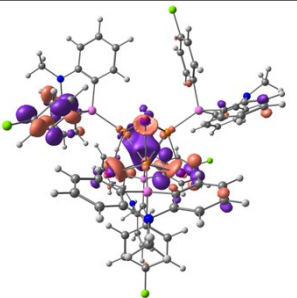
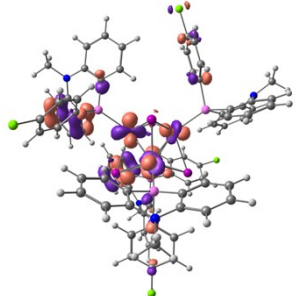
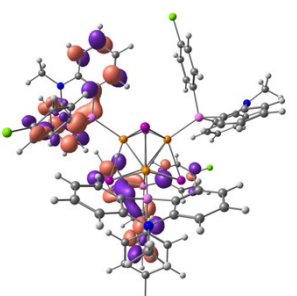
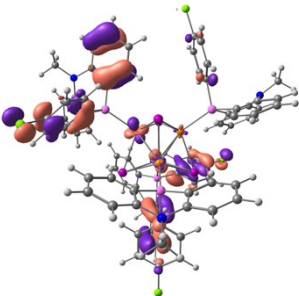
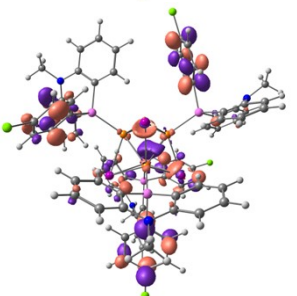
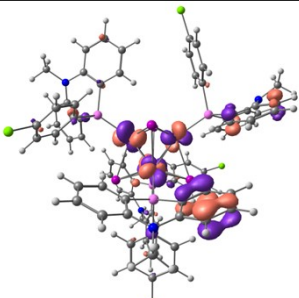
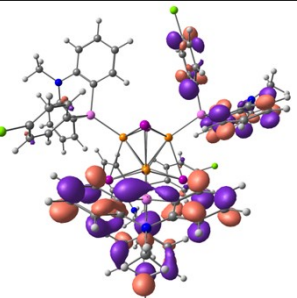
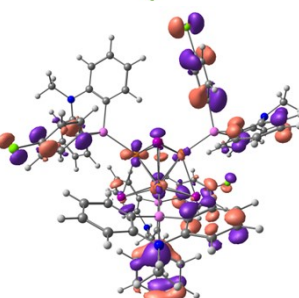
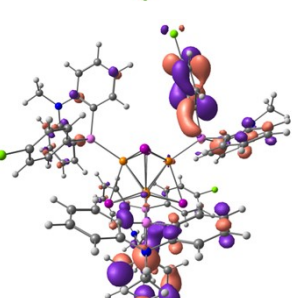
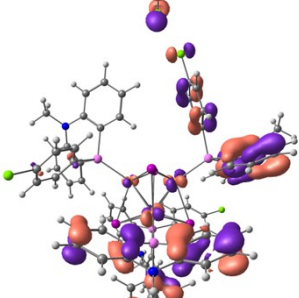
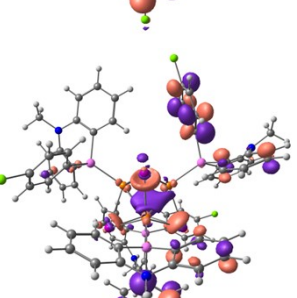
				0.20		
				0.13		
291	0.06	56		0.67		
291	0.06	57		0.67		
284	0.05	81		0.26		
				0.18		

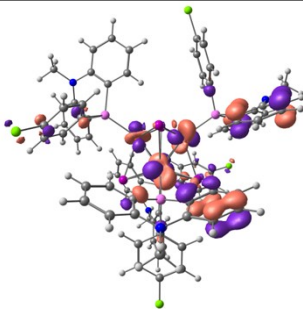
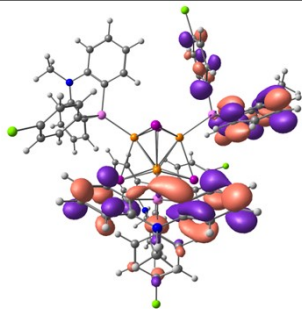
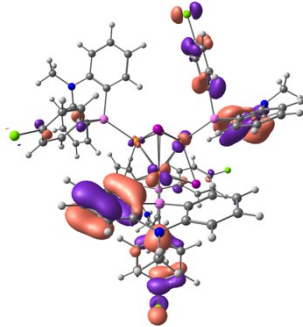
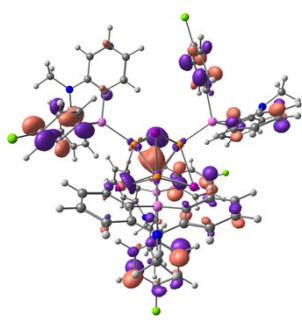
				0.18		
				0.16		
V: ¹ IL	267	0.04	159	0.28		
				0.26		
				0.12		
				0.10		

				0.10		
	265	0.04	171	0.29		
				0.24		
				0.24		
VI: ${}^1\text{IL}$ + ${}^1(\text{X,M})\text{LCT}$ + ${}^1\text{CC}$	231	0.10	360	0.43		
				0.24		

				0.12		
231	0.10	361	0.40	0.21		
			0.12			
230	0.05	372	0.62			

	230	0.05	373	0.62		
	227	0.06	402	0.21		
				0.20		
				0.18		
	221	0.04	456	0.23		
				0.16		

				0.13		
				0.12		
				0.10		
221	0.04	457	0.23			
			0.16			
			0.13			

				0.12		
				0.10		

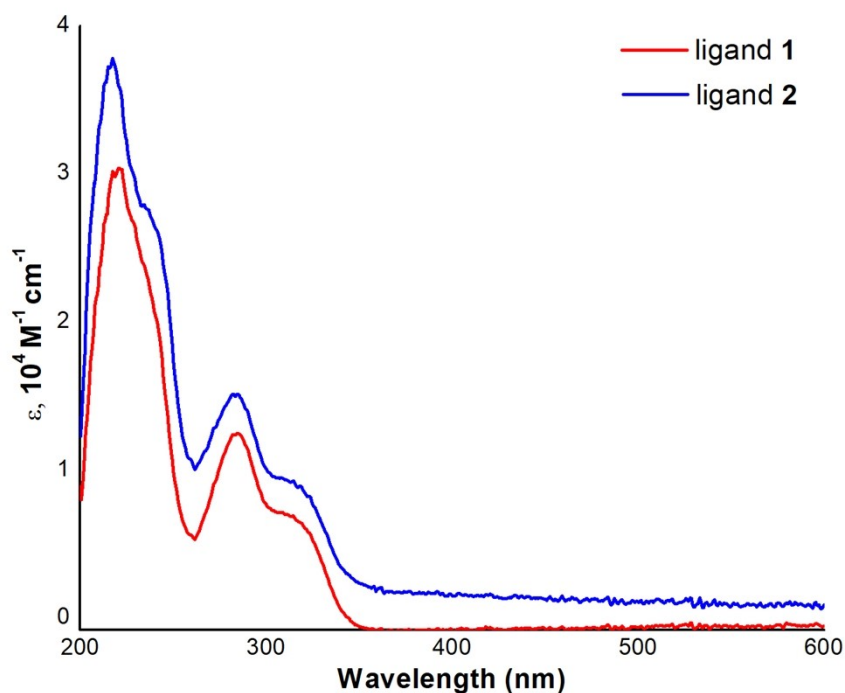


Figure S8. Experimental UV-Vis spectra of ligands **1** and **2** recorded in acetonitrile solution. All measurements were recorded under ambient conditions.

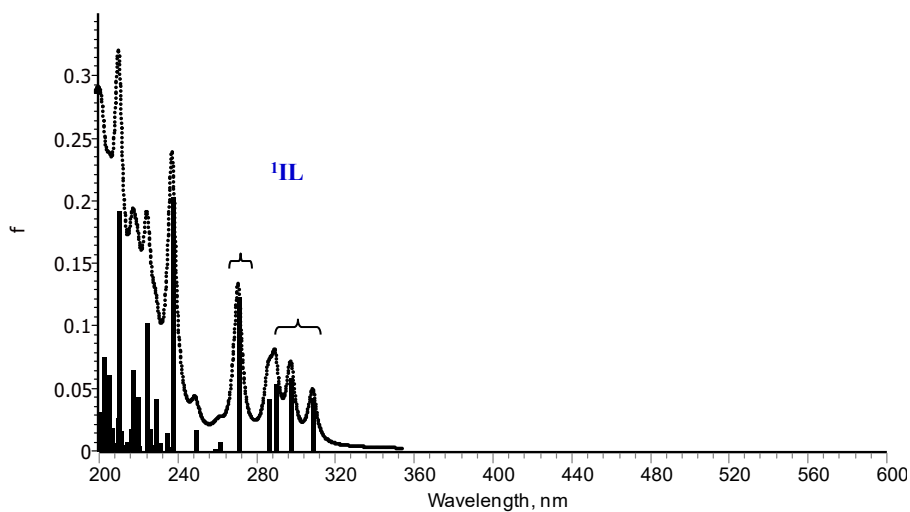


Figure S9. The calculated absorption spectrum for **1**. The vertical lines showing the position of singlet-singlet electronic transitions and their intensity (f – oscillator strength) were broadened by the Lorentz function (f.w.h.m. = 0.25 eV).

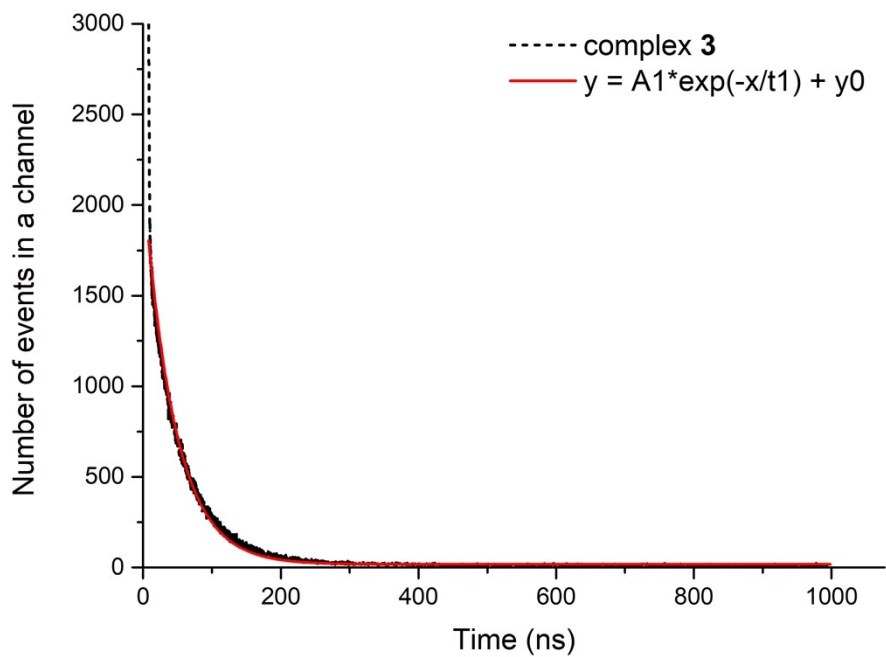


Figure S10. Emission decay curve of the HE band and corresponding fit for complex 3.

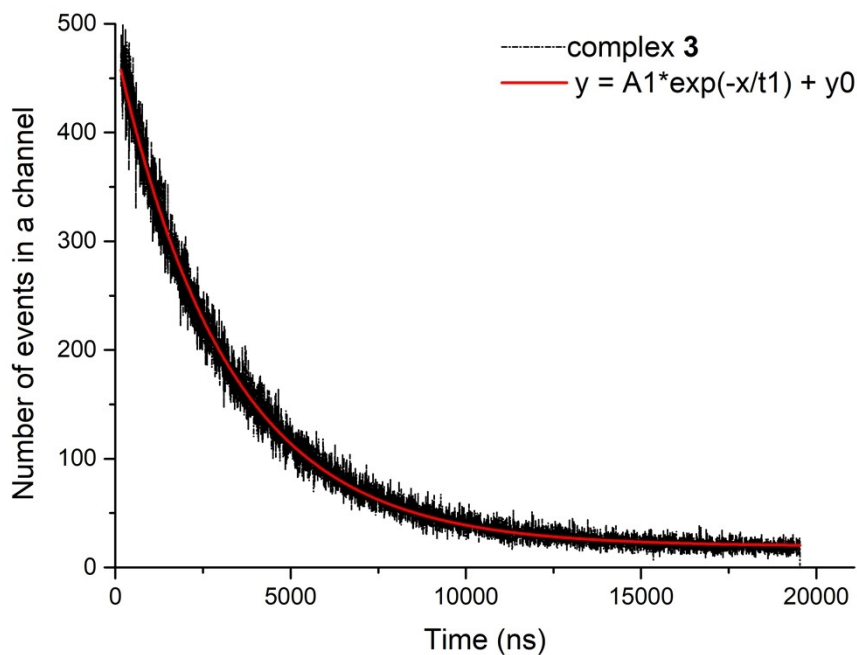


Figure S11. Emission decay curve of the LE band and corresponding fit for complex 3.

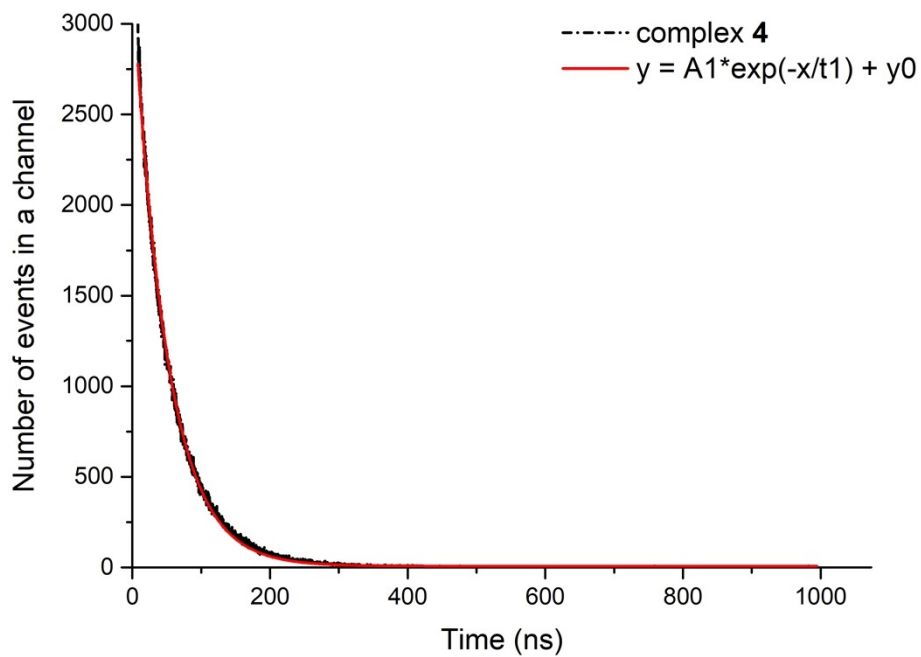


Figure S12. Emission decay curve of the HE band and corresponding fit for complex 4.

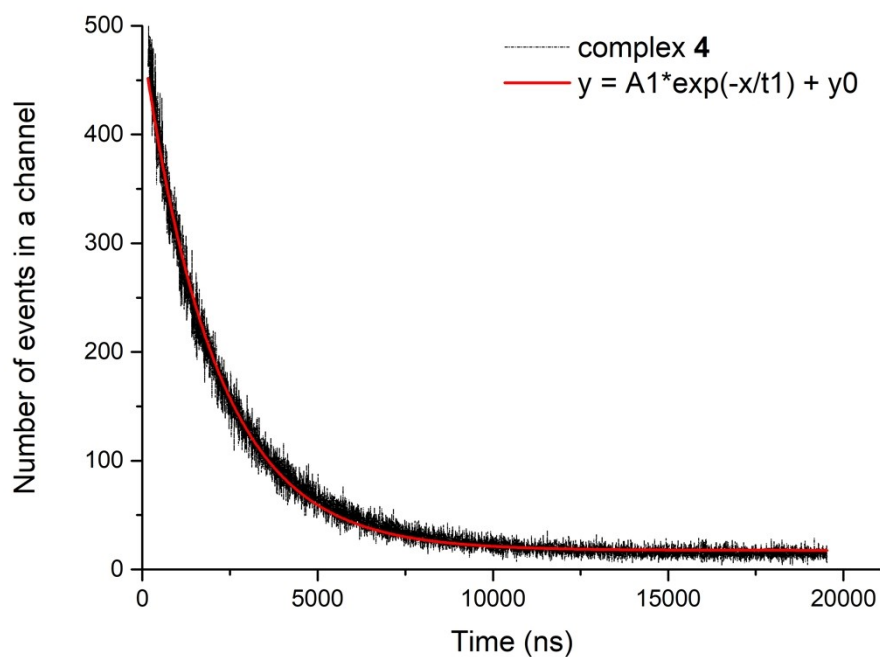


Figure S13. Emission decay curve of the LE band and corresponding fit for complex 4.

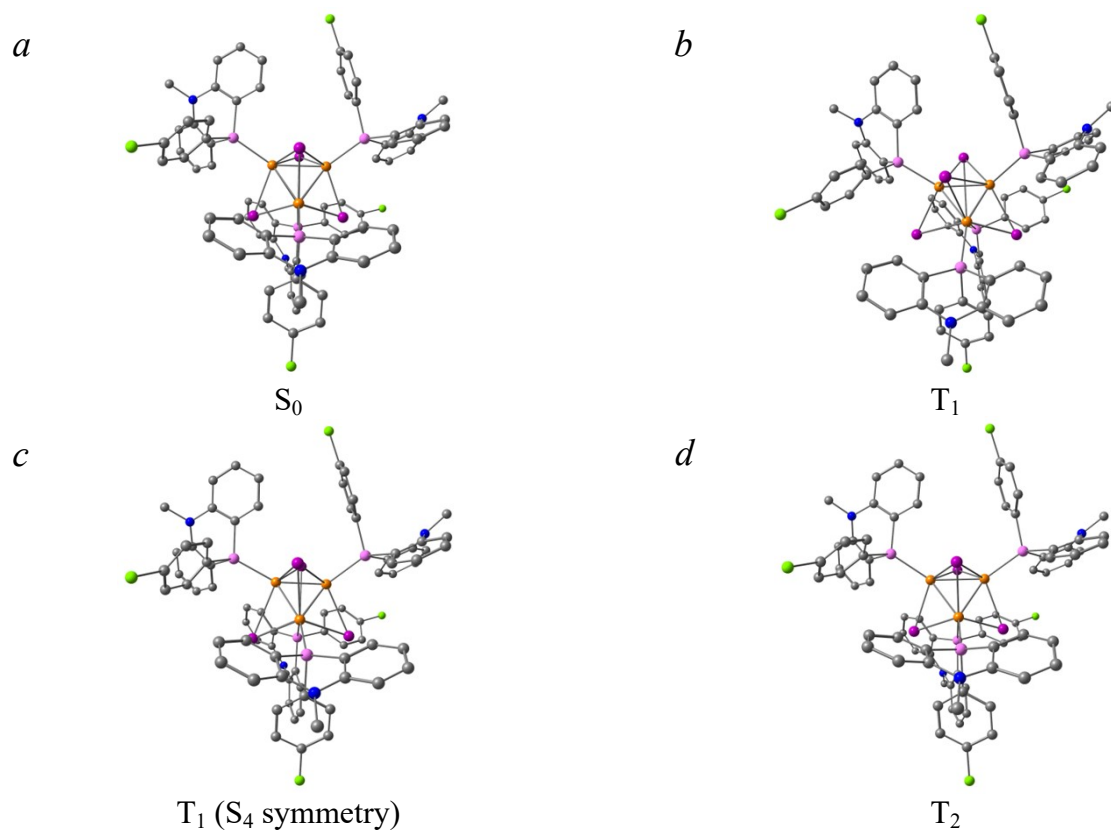


Figure S14. The equilibrium structures of the singlet ground state S_0 (*a*), the lowest triplet state T_1 obtained without (*b*) and with (*c*) accounting for the S_4 symmetry found in the solid state, and the second triplet state T_2 (*d*) (complex **3**).